Electro-diffusion equations of monovalent cations in glass under charge neutrality approximation for optical waveguide fabrication

Xesús Prieto-Blanco
Área de Óptica, Departamento de Física Aplicada,
Escola Universitaria de Óptica e Optometría,
Universidade de Santiago de Compostela,
15782 Galicia, Spain

Abstract

Two improvements of the usual three-dimensional partial differential equations that model ion-exchanged optical devices in glass under charge neutrality approximation are proposed. First, they are rigorously generalised for both non-ideal cation behaviour and concentration-dependent self-diffusion coefficients. Secondly, the Faraday equation is imposed in the derivation instead of the Ohm law. Accordingly, the current density distribution is not governed by the electric field but by the gradient of an effective electrical potential instead. On the other hand, the boundary conditions of those equations are obtained from standard electrolyte theory, which results in contact potentials at interfaces between glass and molten salt, silver film or metallic cathode. Therefore, typical arrangements for field assisted ion exchange must be considered as electrochemical cells, and thus a correction term must be added to the applied voltage to get a proper modelling. This term can be neglected in some typical cases but it must be retained in others. Finally, it is predicted that the electrochemical cell effect can be used to diffuse cations from a silver film without need for an external applied field. This suggests a new simple method to fabricate integrated optical components by ion exchange in glass.

Key words: glass ion-exchange, field-assisted diffusion, electromigration, integrated optics, glass waveguides.
PACS: 66.30.Hs, 66.30.Qa, 42.82.Et, 42.70.Ce

1. Introduction

Ion exchange in glass has been developed and widely applied to fabricate integrated optical devices for more than three decades due to its main advantages: fibre compatibility, low propagation losses and low cost [1,2]. Cations (usually Na^+) close to a glass surface are replaced with other monovalent cations such as K^+, Cs^+, Tl^+ or Ag^+. Molten salts (nitrates) of such cations are common sources of dopants, although a metallic film deposited on the glass surface can be also a source of cations. The exchange happens by thermal movement of cations or it can be assisted by an electric field. The electrical permittivity of the glass (that is the refractive index squared) increases proportionally to the dopant cation concentration and thus, slab optical waveguides can be shaped after a long enough ion exchange. By selective masking of the glass surface, ion exchange can be locally prevented or allowed to fabricate integrated optical elements such as channel waveguides, lenses, total reflection mirrors, splitters, multiplexers and so on. It must be stressed that even amplifiers, lasers and frequency doubling have already been demonstrated in special glasses.

Fibre compatibility, coupling losses between different regions or optical path differences in interference-based devices depend strongly on the refractive index distribution; therefore, the prediction of the cation concentration is of great importance to design high-performance optical devices. Several works have studied the coupled partial differential equations that describe the cation transport [3–11]. The charge neutrality approximation allows an important simplification without relevant loss of accuracy; thus, a drift-diffusion equation and a non standard Laplace equation are obtained in the general case. Section 2 deals with both contributions and limitations of these works in order to make clear why a new study is needed in this topic. The model is generalised to non ideal cation behaviour and concentration-dependent self-diffusion coefficients in Section 3. Moreover, the Faraday's law is included in the new derivation, unlike previous works where the Ohm's law was assumed. This leads to a Laplace equation for an effective

Email address: faxepb@usc.es (Xesús Prieto-Blanco).

electric potential instead of the true electric potential. Although the difference between them amounts at most some tenths of Volt, it must be retained to calculate the electric field.

On the other hand, the boundary conditions of these electro-diffusion equations have received less attention than the equations themselves in the above mentioned works. For example, it is assumed that electric potential is the same at glass surface and at molten salt when they touch each other. Nevertheless, it is known since the sixties that a contact potential exists [12,13]. The exact boundary conditions between salt and glass are obtained in Section 4 from the standard theory of electrolytes [14]. The approach presented in this work results in a new boundary condition at the glass-silver film (anode) interface which presents a contact potential as well. This effect has not been studied yet in the literature. The boundary condition between a metallic cathode and a glass with two cation species at this interface is also studied for the first time.

As regards the new approach, typical arrangements for electro-diffusion are analysed in Section 5. The validity of usual assumptions is discussed; and finally, a new method to fabricate optical waveguides from silver film is suggested.

2. Standard models

The simultaneous diffusion of two cation species (A and B) with different diffusion coefficients (D_A and D_B) in a medium (glass) where fixed anions are present is governed by three second-order coupled partial differential equations: the Poisson's and two drift-diffusion equations (one for each specie of cation). In most cases this system can be simplified under the approximation of charge neutrality, that is, the total cation concentration is assumed to be almost equal to the anion one everywhere. It is supported by the fact that a very small charge disequilibrium is enough to generate a strong electric field which dominates the drift-diffusion equations; this field moves the cations in such a way that the charge neutrality tends to be restored [15,16]. This approximation was developed in [3] for the cases where the total flux of cations ($\vec{J}_0$) is null. Thus, the following diffusion equation (without drift term) is enough to describe the process:

$$\frac{\partial c_A}{\partial t} = \vec{\nabla}\left(\frac{D_A D_B}{D_A c_A + D_B c_B}\vec{\nabla} c_A\right), \tag{1}$$

where t is the time and c_i is the mole fraction of the specie $i = A, B$. Each mole fraction is related with concentrations of both species (C_A and C_B) through:

$$c_i = \frac{C_i}{C_A + C_B} \quad i = A, B. \tag{2}$$

Note that c_B could be eliminated from (1) since $c_A + c_B = 1$, but it is retained for aesthetics. The fraction that appears on the right-hand side of eq. (1) is an inter-diffusion coefficient that depends on both the cation mole fraction and each self-diffusion coefficient; that is, (1) is a non-linear partial equation.

There are interesting processes (such as burying or diffusion from silver film) where a net current crosses the sample. A generalisation of charge neutrality approximation is desirable to describe this kind of cases; it was made for one-dimensional problems in [4], and in the present notation, the following equation was obtained:

$$\frac{\partial c_A}{\partial t} + \frac{D_A D_B}{\left(D_A c_A + D_B c_B\right)^2}\frac{J_{0\mathrm{x}}}{C_0}\frac{\partial c_A}{\partial x} = \frac{\partial}{\partial x}\left(\frac{D_A D_B}{D_A c_A + D_B c_B}\frac{\partial c_A}{\partial x}\right) \tag{3}$$

x being the Cartesian coordinate, C_0 the anion concentration and $J_{0\mathrm{x}}$ the cation flux density along the x-axis. Note that a non-linear drift term proportional to $J_{0\mathrm{x}}$ arises. This one-dimensional flux density does not depend on the position because $\vec{J}_0$ has no sources under charge neutrality approximation (as it will be shown in eq. (17) below).

The generalisation for two or three dimensions has presented much more difficulties than one would expect. Several works have studied this problem with progressive improvements. Thus, a first approach was made in [5] by approximating the total electric field (but not its divergence) by the external one ($\vec{E}_{\mathrm{ext}}$), which leads to:

$$\frac{\partial c_A}{\partial t} + \frac{D_A D_B}{D_A c_A + D_B c_B}\frac{e\vec{E}_{\mathrm{ext}}}{k_{\mathrm{B}}T}\vec{\nabla} c_A = \frac{D_A D_B}{D_A c_A + D_B c_B}\nabla^2 c_A \tag{4}$$

where e, k_{B} and T are the proton charge, the Boltzmann's constant and the absolute temperature respectively; however, this is not a true generalisation, because (1) is not recovered when the external field ($\vec{E}_{\mathrm{ext}}$) is null. This problem was pointed out and overcame in [6] by obtaining the following electro-diffusion equation:

$$\frac{\partial c_A}{\partial t} + \frac{D_A D_B}{D_A c_A + D_B c_B}\frac{e\vec{E}^*_{\mathrm{ext}}}{k_{\mathrm{B}}T}\vec{\nabla} c_A = \vec{\nabla}\left(\frac{D_A D_B}{D_A c_A + D_B c_B}\vec{\nabla} c_A\right). \tag{5}$$

The drift term is again proportional to the field $\vec{E}^*_{\mathrm{ext}}$ defined as:

$$\frac{e\vec{E}^*_{\mathrm{ext}}}{k_{\mathrm{B}}T} = \frac{\vec{J}_0}{D_A C_A + D_B C_B}. \tag{6}$$

Authors of [6] claim that $\vec{E}^*_{\mathrm{ext}}$ is the external applied field, but it will be shown later that charges located inside glass contribute to this field. It must be pointed out that eq. (1) is retrieved if $\vec{E}^*_{\mathrm{ext}} = 0$ into eq. (5). Nevertheless, eq. (3) is not recovered when (5) is reduced to one dimension under the assumption that $\vec{E}^*_{\mathrm{ext}}$ is generated only by charges located outside the glass ($\vec{\nabla}\vec{E}^*_{\mathrm{ext}} = 0$). Specifically, $(E_{\mathrm{ext}})_{\mathrm{x}}$ should be independent of the position in one-dimensional problems

(like J_{0x} above), which makes clear that the drift terms of eqs. (3) and (5) are different although their qualitative behaviour is similar.

On the other hand, both ref. [7] and ref. [8] have obtained the same multi-dimensional electro-diffusion equation:

$$\frac{\partial c_A}{\partial t} + \frac{D_A D_B}{(D_A c_A + D_B c_B)^2} \frac{\vec{J}_0}{C_0} \vec{\nabla} c_A = \vec{\nabla} \left(\frac{D_A D_B}{D_A c_A + D_B c_B} \vec{\nabla} c_A \right) \quad (7)$$

which depends on the total flux density $\vec{J}_0$ instead of the electric field. It can be regarded as a satisfactory extension of both (1) and (3) equations since they are retrieved under proper assumptions. Nevertheless, the problem is shifting now to the $\vec{J}_0$ calculation; note that eq. (17) is not enough for multi-dimensional problems in order to calculate $\vec{J}_0$ in an univocal way. Both ref. [7] and ref. [8] neglected the change of the local conductivity due to the variation of the sample composition; hence, (more or less explicitly) it is assumed that the cation flux is proportional to the external electric field.

The influence of the conductivity change on the flux density has been formalised in ref. [9] to explain why channel waveguides are buried more slowly than slab ones; they assumed the Ohm's law:

$$e\vec{J}_0 = -\sigma \vec{\nabla} V, \quad (8)$$

where V is the electric potential and σ the conductivity related to the mole fractions by means of the following relationship:

$$\sigma = \frac{e^2 C_0}{k_B T} (D_A c_A + D_B c_B). \quad (9)$$

When (8) and (9) are inserted into (17), the following non-standard Laplace equation arises:

$$\vec{\nabla} \left((D_A c_A + D_B c_B) \vec{\nabla} V \right) = 0 \quad (10)$$

which determines V if the concentration profile is known; next $\vec{J}_0$ is trivially calculated from V and it can be substituted into eq. (7) to calculate the c_A evolution. As c_A changes, a recalculation of $\vec{J}_0$ can be needed; that is, two coupled partial differential equations must be solved in the general case. This scheme seems robust, but it will be shown below that a concentration-dependent term must be added to V in the Ohm's law (8) —which will not be assumed but demonstrated— for the sake of consistency with Maxwell's equations.

The above referred works assumed both constant self-diffusion coefficients and ideal behaviours of cations. However, the experimental profile of the field-assisted burying of slab waveguides is much more asymmetric (sharp front of profile and smooth rear tail) than predicted from constant self-diffusion coefficients. A strong dependence of self-diffusion coefficients on cation composition is needed to get an accurate description [17]. Such a dependence is called mixed alkali effect and it has been known for several decades[18–20], although no theory has been universally accepted to explain such effect. Silver and thallium cations in glass behave similarly to alkali ones, so the concept was later extended to mixed mobile ion effect (MMIE). MMIE often stays hidden by the non-linear behaviour of the inter-diffusion coefficient, particularly if no electric field is applied or low mole fractions of incoming cations are used. It explains why the above models predict reasonably the mole fraction in most cases. A mole fraction dependence on D_A and D_B was taken into account in ref. [10] by assuming again the Ohm's law (8), which leads to little changes in eq. (7). Similarly, (5) was directly used in ref. [11] by replacing constant D_i's with concentration-dependent ones, although a rigorous derivation should also include terms depending on $\frac{\partial D_i}{\partial c_A}$. In that work[11], $\vec{E}^*_{\text{ext}}$ was calculated from (10), which is actually equivalent to the procedure of [10] but then $\vec{\nabla} \vec{E}^*_{\text{ext}} \neq 0$.

Both refs. [10] and [11] assumed the flux densities of cations (11) with $g_i = 1$; that is, the behaviour of cations is considered ideal regarding the mole fraction. Nevertheless, experimental works based on ion-exchange equilibrium [21,22] showed a notable deviation from ideality; in that case, the thermodynamic factor g_i must be retained. This factor alters both the inter-diffusion coefficient [23] and the index profile of surface slab waveguides. If self-diffusion coefficients are considered constant and no net current is present ($\vec{J}_0 = 0$), a bump in the central region of the profile is predicted, which agrees with the experiments [24,25]. Later, accurate measurements of diffusion coefficients showed both their dependence on concentration and a non ideal behaviour[26,27].

It must be stressed that there is not a general model including all these phenomena.

3. Derivation of electro-diffusion equations

Equations that describe the most general case of electro-diffusion are derived in this section: multidimensional, field assisted, variable self-diffusion coefficients and non-ideal. Special attention is paid to the application of the charge neutrality approximation without the unnecessary and inaccurate assumption (8).

3.1. *Exact equations*

The flux density of each cation specie ($\vec{J}_i$) is given by:

$$\vec{J}_i = -g_i D_i \vec{\nabla} C_i + D_i C_i \frac{e\vec{E}}{k_B T} \qquad i = A, B \ , \quad (11)$$

where $\vec{E}$ is the electric field, if a_i's are the thermodynamic activities of cations, the thermodynamic factor g_i is defined as:

$$g_i \equiv \frac{\partial \ln a_i}{\partial \ln c_i} \qquad i = A, B. \tag{12}$$

As no cation is destroyed while it diffuses, the continuity equations must be verified, that is:

$$\frac{\partial C_i}{\partial t} + \vec{\nabla} J_i = 0 \qquad i = A, B. \tag{13}$$

Moreover, the Poisson's equation and the Faraday's law of induction must be also fulfilled:

$$\vec{\nabla}(\epsilon \vec{E}) = e(C_A + C_B - C_0) \tag{14}$$

$$\vec{\nabla} \times \vec{E} + \frac{\partial \vec{B}}{\partial t} = 0 \tag{15}$$

where ϵ is the glass electrical permittivity and $\vec{B}$ is the magnetic field which will be assumed as time-independent since the total current changes very slowly.

These six first-order partial derivative equations (from 11 to 15) describe exactly the electro-diffusion of cations.

3.2. *Charge neutrality approximation*

As explained above, a little charge imbalance in (14) generates a strong electric field which gives a dominant contribution to the second term of eq. (11). Moreover, this field tends to balance the charges; for instance, if a region has less cations than anions, it is negatively charged, hence it attracts cations and the neutrality will be retrieved.

The charge neutrality approximation is based on neglecting the electric field divergence in comparison with the charges $e(C_A+C_B)$ and eC_0 in the Poisson's equation (14), which leads to:

$$C_A + C_B = C_0. \tag{16}$$

Now, by adding both continuity equations (13) and using (16), it is obtained:

$$\vec{\nabla} \vec{J}_0 = 0, \tag{17}$$

where the total flux density $\vec{J}_0$ is the addition of both flux densities. Moreover, by adding the flux density equations (11), it is obtained:

$$\begin{aligned} \vec{J}_0 &= \vec{J}_A + \vec{J}_B \\ &= -g_A D_A \vec{\nabla} C_A - g_B D_B \vec{\nabla} C_B \\ &\quad + (D_A C_A + D_B C_B) \frac{e\vec{E}}{k_{\mathrm{B}} T}. \end{aligned} \tag{18}$$

Note the additional diffusion terms compared with Ohm's law (8). By finding the electric field from eq. (18), we have:

$$\frac{e\vec{E}}{k_{\mathrm{B}} T} = \frac{\vec{J}_0}{D_A C_A + D_B C_B} + \frac{g_A D_A \vec{\nabla} C_A + g_B D_B \vec{\nabla} C_B}{D_A C_A + D_B C_B} \tag{19}$$

which will be used twice. On the one hand, the electric field can be substituted in (11) to write the flux density of each cation as a function of $\vec{J}_0$; for instance it leads to:

$$\begin{aligned} \vec{J}_A = &- \frac{(g_B c_A + g_A c_B) D_A D_B}{D_A c_A + D_B c_B} C_0 \vec{\nabla} c_A \\ &+ \frac{D_A c_A}{D_A c_A + D_B c_B} \vec{J}_0, \end{aligned} \tag{20}$$

where (16) has been used again. Next, by inserting eq. (20) into eq. (13) and by taking into account eq. (17), the following electro-diffusion equation is obtained:

$$\begin{aligned} \frac{\partial c_A}{\partial t} + \frac{\partial}{\partial c_A} \left[\frac{D_A c_A}{D_A c_A + D_B c_B} \right] \frac{\vec{J}_0}{C_0} \vec{\nabla} c_A = \\ \vec{\nabla} \left(\frac{(g_B c_A + g_A c_B) D_A D_B}{D_A c_A + D_B c_B} \vec{\nabla} c_A \right). \end{aligned} \tag{21}$$

This equation is an extension of (7) for both non-ideal cation behaviour and concentration-dependent D_i's.

On the other hand, eq. (19) can be inserted into (15) which leads to:

$$\vec{\nabla} \times \left(\frac{\vec{J}_0}{D_A C_A + D_B C_B} \right) = 0 \tag{22}$$

This equation, eq. (17) and the boundary conditions, which will be explained later, determinate the flux density $\vec{J}_0$. From eq. (22), $\vec{J}_0$ can be related to a scalar function ϕ which is much easier to calculate than a vectorial one like $\vec{J}_0$, that is:

$$\frac{\vec{J}_0}{D_A C_A + D_B C_B} = -\frac{e}{k_{\mathrm{B}} T} \vec{\nabla} \phi \tag{23}$$

where the factor $-e/(k_{\mathrm{B}}T)$ was included in order to get for ϕ the same units than the electric potential. Note that $-\vec{\nabla}\phi$ is the same that $\vec{E}^*_{\mathrm{ext}}$ such as defined in eq. (6); nevertheless, they do not verify the standard Laplace equation, in fact, by taking divergences in eq. (23), it is obtained:

$$\frac{e}{k_{\mathrm{B}} T} \nabla^2 \phi = \frac{\partial}{\partial c_A} \left[\frac{D_A c_A}{D_A c_A + D_B c_B} \right] \frac{\vec{J}_0}{C_0} \vec{\nabla} c_A \tag{24}$$

whose result is not zero in general. The partial differential equation of ϕ is obtained by finding $\vec{J}_0$ from eq. (23), taking divergences and using eq. (17):

$$\vec{\nabla} \left((D_A c_A + D_B c_B) \vec{\nabla} \phi \right) = 0, \tag{25}$$

which is the same equation as (10), but the field is ϕ instead of V. To stress the conceptual difference between the present treatment and that of [9], the right equation for V is obtained by taking divergences in eq. (18):

$$\begin{aligned} \vec{\nabla} \left((D_A c_A + D_B c_B) \vec{\nabla} V \right) = \\ -\frac{k_{\mathrm{B}} T}{e} \vec{\nabla} \left(g_A D_A \vec{\nabla} c_A + g_B D_B \vec{\nabla} c_B \right), \end{aligned} \tag{26}$$

which is inhomogeneous (in a mathematical sense) unlike eq. (10). Actually eqs. (25) and (26) are equivalent, but the last one is more difficult to solve, even in one-dimensional problems where the former leads easily to $\vec{J}_0$.

By comparing equations (23) and (25) with (8), (9) and (10), it seems that this mistake between V and ϕ should not have consequences in the calculation of $\vec{J}_0$ and therefore neither should do in c_A. However, in general, the boundary conditions for V and ϕ are a little different. Only in some particular cases they agree, or at least they lead to the same solution for $\vec{J}_0$. In order to obtain the boundary conditions of ϕ, the relationship between ϕ and V is required; it can be easily deduced by replacing eq. (23) into eq. (19) and then integrating:

$$\phi = V + \frac{k_{\mathrm{B}}T}{e}\int_0^{c_A}\left(\frac{D_A c_A \frac{\mathrm{d}\ln a_A}{\mathrm{d}c_A} + D_B c_B \frac{\mathrm{d}\ln a_B}{\mathrm{d}c_A}}{D_A c_A + D_B c_B}\right)\mathrm{d}c_A \quad (27)$$

where the integration limits ensure the equality of ϕ and V for $c_A = 0$. To obtain a more compact equation, the following self-diffusion coefficients are assumed :

$$D_i = D_{ii}\gamma_i \Leftrightarrow D_i c_i = D_{ii} a_i \qquad i = A, B \quad (28)$$

(see appendix), where each $D_{ii} \equiv D_i|_{c_i=1}$ is the self-diffusion coefficient of the corresponding pure specie and γ_i's are the thermodynamic activity coefficients ($a_i = \gamma_i c_i$). This proportionality between activity and diffusion coefficients arises when the energetic level of hopping cations (excited states) are independent of the cation mole fraction. No assumptions are made about the dependence of γ_i's on c_i however. Therefore, eq. (27) can be integrated:

$$\begin{aligned}\phi &= V + \frac{k_{\mathrm{B}}T}{e}\ln\frac{D_A c_A + D_B c_B}{D_{BB}} \\ &= V + \frac{k_{\mathrm{B}}T}{e}\ln\left[\frac{D_{AA}}{D_{BB}}a_A + a_B\right].\end{aligned} \quad (29)$$

It must be stressed that the assumption (28) is not essential, but it simplifies notably the calculations of the next section. From experimental values of D_i's, we can expect that the greater difference between V and ϕ in eq. (29) is about some tenths of Volt, which is negligible in comparison with the usual tensions (between 20 and 100 V) to get optical device fabrication. However, relevant errors in the calculation of the electric field can be made if this difference is ignored. More specifically, the strong gradients of mole fraction occur in the waveguide region, and thus the argument of the logarithm of eq. (29) can change more than one order of magnitude in a few micrometres, which leads to an electric field contribution comparable with a typical external applied field.

Once $\vec{J}_0$ and c_A are known, the charge neutrality approximation can be checked. By taking divergences of both sides of eq. (19), an estimation of charge density is obtained, which can be compared to the total charge of anions $-eC_0$ in eq. (14).

Briefly, the equations to be solved are (21), (23) and (25), whereas (29) will be used in the next section.

4. Boundary conditions

Boundary conditions depend on the substance that is in contact with the glass. Three kinds of substances are usually studied: molten salts, metallic films as cation source and masks. Dielectric and metallic mask are dealt with separately in this work; moreover, metallic film acting as cathode is also studied. The standard theory of electrolytes [14] is applied to obtain the boundary conditions for both c_A and V, in such a way that the usual boundary conditions of c_A are retrieved. When the boundary conditions of V are analysed, it results in a potential difference that arises between the glass and the salt or the metallic film, that is, a contact potential exists when cations can cross the boundary. The boundary condition for ϕ will be obtained from that one for V through (29).

4.1. *Molten salt-glass interface*

The most often used salts are nitrates of sodium, potassium and silver, or mixtures of them. [28–33]

4.1.1. *One specie of cations*

The simplest case occurs when only one cation specie is present both in glass and salt (e.g. sodium cations). These cations move from salt to glass and vice versa to achieve the equilibrium, which happens when the cation electrochemical potentials are equal in both phases and they do not depend on the position, that is:

$$\mu^0_{B\mathrm{s}} = \mu^0_B \qquad (B_{\mathrm{s}} \leftrightarrow B) \quad (30)$$

where the subindex 's' means the salt, no subindex means the glass and the super-index '0' means that no A cation is present. The chemical equation is also included in parenthesis. As cations are charged particles, each electrochemical potential can be split into an electrical and a chemical part:

$$\begin{aligned}\mu^0_B &= \bar{\mu}^0_B(C_B) + eV, \\ \mu^0_{B\mathrm{s}} &= \bar{\mu}^0_{B\mathrm{s}}(C_{B\mathrm{s}}) + eV_{\mathrm{s}}.\end{aligned} \quad (31)$$

Therefore:

$$e(V_{\mathrm{s}} - V) = \bar{\mu}^0_B(C_B) - \bar{\mu}^0_{B\mathrm{s}}(C_{B\mathrm{s}}). \quad (32)$$

Note that $\bar{\mu}^0_B(C_B)$ and $\bar{\mu}^0_{B\mathrm{s}}(C_{B\mathrm{s}})$ can depend on the position through C_B and $C_{B\mathrm{s}}$ respectively; of course V and V_{s} also depend on the position in such a way that μ^0_B and $\mu^0_{B\mathrm{s}}$ remain homogeneous.

Although the dependence of the chemical potentials on the respective concentrations is unknown, the problem can be analysed from a qualitative viewpoint. Let us suppose that the salt has less energetic states which results in a lower value of its chemical potential in bulk region; thus, if both phases are put into contact, glass cations tend to cross the interface. As cations cross, a negative charge builds up

in the glass and a positive one also appears in the salt. The resultant electrostatic force keeps these charges confined in two thin surface layers (typically some nanometres thick). These charges cause a potential difference between the glass and the molten salt. Obviously, the cation migration stops when this difference balances the original energetic step. This contact potential is similar to the one that occurs between two metals or in a P-N semiconductor junction.

Hereafter, the thickness of these charged layers will be neglected, but the potential difference will be retained by evaluating the electrochemical potentials near the boundary but far enough to just avoid charged layers; this is formalised by using the subindex '$|_{\mathrm{F}}$' as follows:

$$V|_{\mathrm{F}} = V_{\mathrm{s}} + \frac{\bar{\mu}^0_{B\mathrm{s}} - \bar{\mu}^0_B}{e} \tag{33}$$

where the dependence on the concentration of chemical potentials was removed to indicate that its values are referred to the bulk region where $C_B \approx C_0$. It must be stressed that (33) remains valid although a weak disequilibrium was present (for example when an electric current crosses the boundary) because the continuity of the electrochemical potential at the frontier can be assumed; this means, local equilibrium still exits. Likewise, the bulk value of the salt potential (V_s) is used instead of its value at the surface ($V_s|_{\mathrm{F}}$) because the conductivity of the molten salt is much higher than that of the glass, hence the potential differences into the salt can be neglected. In brief, the charge density near the interface is not neglected, but the thickness of the charged region is.

Finally, the boundary condition of ϕ is equal to that of V because $c_A = 0$:

$$\phi|_{\mathrm{F}} = V_{\mathrm{s}} + \frac{\bar{\mu}^0_{B\mathrm{s}} - \bar{\mu}^0_B}{e} \tag{34}$$

4.1.2. *Two species of cations*

Although the electrochemical potentials also depend on the mole fractions of cations when two species are present, the above method can be applied to each specie:

$$\begin{aligned} \mu_{A\mathrm{s}} &= \mu_A|_{\mathrm{F}} \qquad (A_{\mathrm{s}} \leftrightarrow A) \\ \mu_{B\mathrm{s}} &= \mu_B|_{\mathrm{F}} \qquad (B_{\mathrm{s}} \leftrightarrow B). \end{aligned} \tag{35}$$

Note that the bulk value of the electrochemical potentials was used in the salt phase. The salt can be assumed as homogeneous (the same mole fraction everywhere) because its cation mobility is much higher than the one in glass; moreover, the salt convection continuously renews the salt at the boundary. By splitting the electrochemical potentials, it is obtained:

$$\begin{aligned} \bar{\mu}_{A\mathrm{s}} + eV_{\mathrm{s}} &= \bar{\mu}_A|_{\mathrm{F}} + eV|_{\mathrm{F}} \\ \bar{\mu}_{B\mathrm{s}} + eV_{\mathrm{s}} &= \bar{\mu}_B|_{\mathrm{F}} + eV|_{\mathrm{F}}. \end{aligned} \tag{36}$$

The electric potentials vanish by subtracting both equations which leads to:

$$\bar{\mu}_{A\mathrm{s}} + \bar{\mu}_B|_{\mathrm{F}} = \bar{\mu}_A|_{\mathrm{F}} + \bar{\mu}_{B\mathrm{s}} \qquad (A_{\mathrm{s}} + B \leftrightarrow A + B_{\mathrm{s}}), \tag{37}$$

but as neither salt nor glass behave ideally, then:

$$\left.\begin{aligned} \bar{\mu}_i &= \bar{\mu}^0_i + k_{\mathrm{B}}T \ln a_i \\ \bar{\mu}_{i\mathrm{s}} &= \bar{\mu}^0_{i\mathrm{s}} + k_{\mathrm{B}}T \ln a_{i\mathrm{s}} \end{aligned}\right\} \qquad i = A, B; \tag{38}$$

therefore:

$$\ln \frac{a_{A\mathrm{s}} a_B|_{\mathrm{F}}}{a_{B\mathrm{s}} a_A|_{\mathrm{F}}} = \frac{\bar{\mu}^0_A - \bar{\mu}^0_{A\mathrm{s}} - (\bar{\mu}^0_B - \bar{\mu}^0_{B\mathrm{s}})}{k_{\mathrm{B}}T}. \tag{39}$$

To relate mole fractions at the glass boundary ($c_A|_F$ and $c_B|_F$) with those of salt ($c_{A\mathrm{s}}$ and $c_{B\mathrm{s}}$), some authors [21,22] applied both the regular mixture model to salt (see [34] for experimental values of W_s):

$$\ln a_{i\mathrm{s}} = \ln c_{i\mathrm{s}} + \frac{W_s}{k_{\mathrm{B}}T}(1 - c_{i\mathrm{s}})^2 \qquad i = A, B, \tag{40}$$

and the experimental law [35]:

$$\frac{a_B}{a_A} = \left(\frac{c_B}{c_A}\right)^n \tag{41}$$

(n being a constant) to the ratio of the thermodynamic activities in glass. Thus (39) fixes c_A at the glass frontier, therefore it is a Dirichlet boundary condition.

Once mole fractions at the glass boundary are known, the contact potential is fixed by any equation from (36):

$$\begin{aligned} V|_{\mathrm{F}} &= V_{\mathrm{s}} + \frac{\bar{\mu}^0_{A\mathrm{s}} - \bar{\mu}^0_A}{e} + \frac{k_{\mathrm{B}}T}{e} \ln \frac{a_{A\mathrm{s}}}{a_A|_{\mathrm{F}}} \\ &= V_{\mathrm{s}} + \frac{\bar{\mu}^0_{B\mathrm{s}} - \bar{\mu}^0_B}{e} + \frac{k_{\mathrm{B}}T}{e} \ln \frac{a_{B\mathrm{s}}}{a_B|_{\mathrm{F}}}, \end{aligned} \tag{42}$$

and thus the following Dirichlet condition for ϕ is obtained:

$$\begin{aligned} \phi|_{\mathrm{F}} &= V_{\mathrm{s}} + \frac{\bar{\mu}^0_{A\mathrm{s}} - \bar{\mu}^0_A}{e} + \frac{k_{\mathrm{B}}T}{e} \ln \left[a_{A\mathrm{s}} \left(\frac{a_B|_F}{a_A|_F} + \frac{D_{AA}}{D_{BB}} \right) \right] \\ &= V_{\mathrm{s}} + \frac{\bar{\mu}^0_{B\mathrm{s}} - \bar{\mu}^0_B}{e} + \frac{k_{\mathrm{B}}T}{e} \ln \left[a_{B\mathrm{s}} \left(1 + \frac{D_A c_A}{D_B c_B} \right)_{\mathrm{F}} \right]. \end{aligned} \tag{43}$$

Note that $c_A|_{\mathrm{F}}$ is the same in all points of the glass surface in contact with the salt. Therefore, both $V|_{\mathrm{F}}$ and $\phi|_{\mathrm{F}}$ are also constant along the frontier between salt and glass, but different from V_{s}.

4.2. *Metallic film as a cation source*

Silver [36–43] and, to a lesser extent, copper [44,45] are the metals used as cation sources. Introduction of both gold and cobalt from metal films has been recently demonstrated although their diffusion coefficients are so low that neutrality charge approximation fails [46].

In theory, the atoms of the film (called A) can enter into the glass as cations, and glass cations (both A and B) can be adsorb to the film, therefore equations like (35) apply:

$$\begin{aligned} \mu_{A^+\mathrm{f}} &= \mu_A|_{\mathrm{F}} \qquad (A_{\mathrm{f}} \leftrightarrow A) \\ \mu_{B^+\mathrm{f}} &= \mu_A|_{\mathrm{F}} \qquad (B_{\mathrm{f}} \leftrightarrow B) \end{aligned} \tag{44}$$

Table 1
Melting point (°C), work functions, ionisation and cohesive energies (eV) used to estimate $W^A_{A^+}$ of several elements.

	T_{melt}	Cohesive energy (W^A_A) at 0 K [47]	Ionisation energy (I_A) [47]	Work function ($W^A_{e^-}$) [47]	Work function ($W^A_{e^-}$) [48]	$W^A_{A^+}$
Li	180	1.63	5.39		2.38	4.64
Na	98	1.113	5.14		2.35	3.90
K	64	0.934	4.34		2.22	3.05
Rb	39	0.852	4.18		2.16	2.87
Cs	29	0.804	3.89	2.14[a]	1.81	2.72
Cu	1083	3.49	7.72	4.59 4.48 4.98[b]	4.4	6.7
Ag	961	2.95	7.57	4.64 4.52 4.74[b]	4.3	6.1
Tl	304	1.88	6.11		3.7	4.29

[a] polycrystalline; [b] depending on the crystallographic face

where $\mu_{A^+\text{f}}$ and $\mu_{B^+\text{f}}$ are the electrochemical potentials of cations in silver film [1]. Nevertheless, as alkalies form very unstable metals, the second equation is strongly shifted to the right; that is the amount of B cations adsorbed to the film is usually so small that it can be neglected. In other words, it is assumed that B specie can not cross the boundary. Thus, the second equation (44) can be replaced with the simpler one:

$$\vec{J}_B|_{\text{F}} \cdot \hat{e}_{\text{F}} \cong 0 \tag{45}$$

where $\hat{e}_{\text{F}}$ is the unit normal vector of the boundary that faces the glass. This condition is equivalent to:

$$\vec{J}_A|_{\text{F}} \cdot \hat{e}_{\text{F}} \cong \vec{J}_0|_{\text{F}} \cdot \hat{e}_{\text{F}} \tag{46}$$

which leads to the following relationship:

$$\vec{\nabla} c_A|_{\text{F}} \cdot \hat{e}_F \cong -\left[\frac{c_B}{g_B c_A + g_A c_B}\right]_{\text{F}} \frac{\vec{J}_0|_{\text{F}} \cdot \hat{e}_{\text{F}}}{D_A|_{\text{F}} C_0}. \tag{47}$$

This equation is a mixed boundary condition for c_A because it relates c_A to its normal derivative. The condition (47) is enough to solve one-dimensional problems where J_0 is fixed externally; nevertheless, more general problems require the use of the first equation from (44). As B cations are hardly present in the metal, $\mu_{A^+\text{f}}$ does not depend on the concentration and it can be approximated as:

$$\mu_{A^+\text{f}} = -W^A_{A^+} + eV_{\text{f}}, \tag{48}$$

$W^A_{A^+}$ being the energy necessary to extract a cation from the metal. It can be calculated from the ionisation energy of a free atom (I_A), the cohesive energy (W^A_A) and the work function of the metal ($W^A_{e^-}$) by the following relationship:

$$W^A_{A^+} + W^A_{e^-} = W^A_A + I_A \tag{49}$$

[1] In this phase it is necessary to distinguish between $\mu_{A^+\text{f}}$ and $\mu_{A\text{f}}$ where the latter is the chemical potential of *neutral* atoms in the film. In both glass and molten salt phases, only the electrochemical potential of cations is used, so the sign '+' was omitted for brevity.

Its value for silver ($W^{\text{Ag}}_{\text{Ag}^+}$) can be considered as independent of the temperature for the present purposes since the thermal energy of metallic silver at 600 K can be bounded in 0.16 eV per atom from Dulong et Petit law, which is lower than the $W^{\text{Ag}}_{e^-}$ accuracy at 0 K. The variation of the work function is even lower (~ 0.4 meV) within this temperature range. Similar calculations can be made for alkaline metals (table 1), although in these cases the heat of fusion must be also neglected (10 meV). Based on these considerations, it is obtained:

$$V|_{\text{F}} = V_{\text{f}} + \frac{-W^A_{A^+} - \bar{\mu}^0_A}{e} - \frac{k_{\text{B}}T}{e} \ln a_A|_{\text{F}}. \tag{50}$$

Now, $V|_{\text{F}}$ can depend on the considered frontier point through $a_A|_{\text{F}}$ since (47) does not fix the value of $c_A|_{\text{F}}$ unlike (39). Like in the equation (29), the term proportional to $k_{\text{B}}T/e$ is small but its derivative along the boundary can not be neglected if the gradient of the mole fraction has a large tangential component. In this case, the electric field has also that component. Note that the electric field is not present at the metal surface but at the glass surface; this discontinuity arises from the dependence of the contact potential on the position. This is explained differently as follows: as $\mu_A|_{\text{F}} = \mu_{A^+\text{f}} = eV_{\text{f}} - W^A_{A^+}$, μ_A is a constant along the boundary, therefore the flux density of A cations is normal to it:

$$\vec{J}_A|_{\text{F}} \times \hat{e}_{\text{F}} = 0 \tag{51}$$

If $\vec{\nabla} c_A|_{\text{F}} \times \hat{e}_{\text{F}} \neq 0$ a tangential diffusive flux occurs, then a tangential component of the electric field must also occur to cancel it, and thus to preserve the condition given by the eq. (51). This equation can be deduced from eq. (50) by taking derivatives, but an additive constant is lost; therefore the inverse claim is not true.

By using (50) and (29), a Dirichlet condition for ϕ is obtained:

$$\phi|_{\text{F}} = V_{\text{f}} + \frac{-W^A_{A^+} - \bar{\mu}^0_A}{e} + \frac{k_{\text{B}}T}{e} \ln\left[\frac{D_{AA}}{D_{BB}} + \frac{a_B|_{\text{F}}}{a_A|_{\text{F}}}\right], \tag{52}$$

Again, a change of c_A along the boundary implies that ϕ also depends on the point; then, in its turn, the total flux density has a tangential component through (23). As $\vec{J}_A$ is normal to the boundary, only B cations contribute to the tangential component of $\vec{J}_0$. Furthermore, $\vec{J}_B$ has not a normal component —see (45)—. Therefore $\vec{J}_A$ is normal to the interface glass-film whereas $\vec{J}_B$ is tangent and proportional to the variation of the mole fraction along this interface.

To my knowledge, the boundary conditions (50), (51) and (52) have not been previously reported.

4.3. *Metallic film as a cathode*

A metallic film (Al [36,37,39,41], Ag [42,43], Cu [38]) deposited on the back side of the sample is often used in electro-migration process as a cathode. When the current crosses the sample, cations from glass reduce to metal and

Table 2
Miscibility of some metals in the 200°C-500°C range. [49,50]

	Na	K	Rb	Cs	Tl	Al	Ti	Cr	Cu	Ag
Li	r, 1-2	i	i	i	r, 3-8	r, 4-5	i	i	r, 2	r, 2-5
Na		m	m	m	r, 1-4	i	i	i	i	r, 2-3
K			m	m	r, 1-6	i	i	i	–	–
Rb				m	r, 1-6	–	i	i	–	–
Cs					r, 1-6	i	i	i	i	–
Tl						i	–	–	i	r, 2-3

m: miscible; i: immiscible or insoluble; r, $n_{\min}$-$n_{\max}$: miscible or soluble only in some regions of the phase diagram, being $n_{\min}$ and $n_{\max}$ the minimum and maximum number of phases that can be obtained by varying the concentration at constant temperature in the range 200°C to 500°C; –: not available.

form a build-up layer under the film. At usual fabrication temperatures alkali metals are melted (Table 1) and they form alloys with some other metals. For example, gold dissolves into molten potassium or they can form a sequence of four intermetallic compounds depending on their relative concentration [49, Vol I]. So, a thick film seems advisable when these metals are used. In contrast, Al, Ti or Cr have negligible miscibility with most alkalies (Table 2), although tendency to deterioration of Al has been reported[2, Chapter 3]. Next, these non-soluble films are discussed.

If the backside of the sample contents only one cation specie, one equation like (34) must simply be applied to calculate the boundary condition of ϕ. In contrast, a lot of different situations can occur when two species are present.

4.3.1. *Two alkalies present near the cathode*

As alkalies (lithium excepted) are miscible with each other (Table 2), equations similar to (39) and (43) must be used if the glass has two alkalies among Na, K, Rb and Cs (for instance BK7 glass contents Na and K). Thus, if pure alkali metals are chosen as the reference states, the electrochemical potentials ($\mu_{i^+\mathrm{l}}$) in the layer are:

$$\mu_{i^+\mathrm{l}} = -W^i_{i^+} + k_\mathrm{B}T \ln a_{i\mathrm{l}} + eV_\mathrm{l} \qquad i = A, B \ , \tag{53}$$

where the subindex 'l' refers to the layer, this means that $a_{i\mathrm{l}}$ is the activity of the cation $i = A, B$ in the layer. Thus the equation equivalent to (39) is:

$$\ln \frac{a_{A\mathrm{l}} a_B|_\mathrm{F}}{a_{B\mathrm{l}} a_A|_\mathrm{F}} = \frac{\bar{\mu}^0_A + W^A_{A^+} - (\bar{\mu}^0_B + W^B_{B^+})}{k_\mathrm{B}T} \equiv \ln K_\mathrm{l} \ , \tag{54}$$

where K_l is the equilibrium constant of the chemical reaction $A_\mathrm{l} + B \leftrightarrow A + B_\mathrm{l}$.

Unlike ion exchange from molten salts, there is not a huge reservoir of cations outside of glass that keeps the boundary conditions constant. The alkali layer composition rather depends on the amount of each cation specie that had crossed the boundary from the process start ($t = 0$). As the instantaneous contributions ($\vec{J}_i|_\mathrm{F} \cdot \hat{e}_\mathrm{F}$) can change with time, the alkali mole fractions in the layer ($c_{i\mathrm{l}}$) also can change. If both $\vec{J}_A|_\mathrm{F}$ and $\vec{J}_B|_\mathrm{F}$ are homogeneous along the glass-cathode interface, it is clear that:

$$c_{i\mathrm{l}} = \frac{\int_0^t \vec{J}_i|_\mathrm{F} \cdot \hat{e}_\mathrm{F} \, \mathrm{d}t'}{\int_0^t \vec{J}_0|_\mathrm{F} \cdot \hat{e}_\mathrm{F} \, \mathrm{d}t'} \qquad i = A, B. \tag{55}$$

As $a_{i\mathrm{l}}$ depends on $c_{i\mathrm{l}}$, the boundary condition for glass mole fraction ($c_A|_\mathrm{F}$) changes with time through eq. (54), which alters again the flux densities $\vec{J}_i$'s and so on. Note that $\vec{J}_0$ also changes with time through $\phi|_\mathrm{F}$, but usually to a lesser extent. It is worth saying that the following relationship is verified at the initial instant:

$$\left.\frac{c_{A\mathrm{l}}}{c_{B\mathrm{l}}}\right|_{t=0} = \left.\frac{\vec{J}_A|_\mathrm{F} \cdot \hat{e}_\mathrm{F}}{\vec{J}_B|_\mathrm{F} \cdot \hat{e}_\mathrm{F}}\right|_{t=0}, \tag{56}$$

When (56) is inserted into (54), it is obtained:

$$\left[\frac{\gamma_{A\mathrm{l}}}{a_A|_\mathrm{F}} \, \vec{J}_A|_\mathrm{F} \cdot \hat{e}_\mathrm{F}\right]_{t=0} = K_\mathrm{l} \left[\frac{\gamma_{B\mathrm{l}}}{a_B|_\mathrm{F}} \, \vec{J}_B|_\mathrm{F} \cdot \hat{e}_\mathrm{F}\right]_{t=0}. \tag{57}$$

4.3.2. *Silver and sodium present near the cathode*

Special attention must be paid if the diffusing species are silver and sodium, say A and B respectively. They are immiscible as metals for a wide composition range, although a little amount of silver is soluble in molten sodium. Its saturation mole fraction —$c^{\max}_{\mathrm{Ag\,l}}(T)$— ranges from 0.2% to 5% approximately when the temperature is between 200°C and 500°C. Moreover, a solid intermetallic compound (Ag_2Na) is stable up to 322°C[49, Vol. I]. Therefore, three different regimes are possible above 322°C. The first occurs when a relevant amount of silver is present at the glass back surface, for example if the sample was previously silver-exchanged. In this case, only metallic silver is present in the cathode because sodium cations can not leave the glass as it was explained in section 4.2. Hence boundary conditions (47) and (52) remain valid. Nevertheless, as only silver cations leave the glass, their mole fraction at surface ($c_{\mathrm{Ag}}|_\mathrm{F}$) reduces with time which increases the contact potential ($V|_\mathrm{F} - V_\mathrm{f}$) as eq. (52) shows. The silver depletion stops at an extremely low mole fraction, when the contact potential is large enough to force the sodium cations to leave the glass and to form a molten layer of silver-saturated metallic sodium. In this moment the second regime starts: the eqs. (45) and (47) are no longer valid. Now, the situation is similar to that of the section 4.3.1 although the eq. (53) does not apply to silver cations since their mole fraction is limited up to $c^{\max}_{\mathrm{Ag\,l}}(T)$. The silver saturated mixture is a good reference state since metallic and saturating silver cations are in equilibrium; so the electrochemical potential of silver cations in a non-saturated layer is:

$$\mu_{\mathrm{Ag}^+\mathrm{l}} = -W^{\mathrm{Ag}}_{\mathrm{Ag}^+} + k_\mathrm{B}T \ln \frac{a_{\mathrm{Ag\,l}}}{c^{\max}_{\mathrm{Ag\,l}}} + eV_\mathrm{l} \ , \tag{58}$$

where the silver activity in the layer $a_{\mathrm{Ag\,l}}$ meets the silver mole fraction when it is saturated: $a_{\mathrm{Ag\,l}}(c^{\max}_{\mathrm{Ag\,l}}) = c^{\max}_{\mathrm{Ag\,l}}$. Therefore, the following expression is obtained for both saturated and non-saturated layer:

$$k_\mathrm{B}T \ln \left.\frac{a_{\mathrm{Ag}}}{a_{\mathrm{Na}}}\right|_\mathrm{F} = (\bar{\mu}^0_{\mathrm{Na}} - \bar{\mu}^0_{\mathrm{Ag}}) + (W^{\mathrm{Na}}_{\mathrm{Na}^+} - W^{\mathrm{Ag}}_{\mathrm{Ag}^+})$$

$$+ k_{\mathrm{B}}T \ln \frac{a_{\mathrm{Ag\,l}}/c_{\mathrm{Ag\,l}}^{\max}}{a_{\mathrm{Na\,l}}} \tag{59}$$

For a saturated layer, the last term amounts less than 4 meV since $0.95 \leq c_{\mathrm{Na\,l}} \leq 1$ and it can be ignored compared with the second term in parenthesis which amounts –2.2 eV. The first term in parenthesis is unknown because it depends on the glass composition, but probably it is also a negative quantity because sodium cations are smaller than silver cations, which allows more stable bond with SiO^- anions. But even if the first parenthesis is neglected, the eq. (59) leads to a very low boundary condition for silver mole fraction in glass:

$$c_{\mathrm{Ag}}|_{\mathrm{F}} < O(10^{-14}) \simeq 0 \quad \Rightarrow \quad c_{\mathrm{Na}}|_{\mathrm{F}} \simeq 1 \tag{60}$$

and then the boundary conditions for V and ϕ are obtained by using the eq. (53) for sodium:

$$\phi|_{\mathrm{F}} = V|_{\mathrm{F}} = V_{\mathrm{l}} - \frac{\bar{\mu}^0_{\mathrm{Na}} + W^{\mathrm{Na}}_{\mathrm{Na^+}}}{e}. \tag{61}$$

Note that silver cations continue leaving the sample in spite of condition (60) while $\vec{\nabla} c_{\mathrm{Ag}}|_{\mathrm{F}} \cdot \hat{e}_{\mathrm{F}} > 0$ —see eq. (20)—.

The third regime is achieved when the supplied sodium is enough to fully dilute the metallic silver, that is, when the layer becomes non-saturated. The difference between the second and the third regime is rather formal since the boundary conditions (60) and (61) remain valid; they are even more accurate if silver is more diluted —see eq. (59)—.

Below 322°C the second regime splits in two: the formation of a solid layer of Ag_2Na in presence of metallic silver and the build-up of a molten layer of silver-saturated sodium in presence of Ag_2Na. The limited temperature range of Ag_2Na existence indicates that this compound is not very stable which suggests that conditions (60) and (61) are also valid in the new regimes.

In case of copper and sodium presence near the cathode, an analogous treatment as the above one would be applied but the second regime does not exist since copper and sodium are practically immiscible.

4.4. *Dielectric masks*

A mask is a substance deposited on the glass (preferably without pinholes or other piercing defects [51]) in order to avoid that any cation crosses the glass frontier even if the glass sample is immersed in molten salt. Same conditions also apply to any glass surface in contact with air. If the mask is a dielectric like Al_2O_3[52], SiO_2, Si_3N_4, polyimide [51] or photoresist[43] no charge transference is possible between cations and mask, thus:

$$\begin{aligned} \vec{J}_A|_{\mathrm{F}} \cdot \hat{e}_{\mathrm{F}} &= 0 \\ \vec{J}_B|_{\mathrm{F}} \cdot \hat{e}_{\mathrm{F}} &= 0 \end{aligned} \tag{62}$$

It leads to Newman conditions for c_A, V and ϕ:

$$\vec{\nabla} c_A|_{\mathrm{F}} \cdot \hat{e}_{\mathrm{F}} = 0 \tag{63}$$

$$\vec{\nabla} V|_{\mathrm{F}} \cdot \hat{e}_{\mathrm{F}} = 0 \tag{64}$$

$$\vec{\nabla} \phi|_{\mathrm{F}} \cdot \hat{e}_{\mathrm{F}} = 0 \tag{65}$$

4.5. *Metallic masks*

Aluminium [37–39,51–54] or titanium [39,51,54–56] films are widely used as metallic mask; Cr masks have been also proposed for dry field-assisted ion exchange [41]. Their boundary conditions have been also modelled by the eq. (62) in the literature, in spite of several known failures of the model. First, silver reduction occurs at the edges of aluminium masks while Ag^+/Na^+ thermal ion exchange is carried out, which results in large propagation losses of channel waveguides fabricated like that [52]. Secondly, the index distribution beneath the aluminium mask is not the one expected from (62) both for Ag^+/Na^+ [52] and K^+/Na^+ [53] thermal ion exchange. More specifically, the depth of channel waveguides saturates whereas its side diffusion continues, resulting in channels with large aspect ratios (≥ 2.2) which hinders light coupling to optical fibres [57]. When the mask becomes dielectric by aluminium anodising, these failures are removed [52], that is why they have been qualitatively related to electrochemical potentials and electric fields under the mask. Finally, a transitory current flows through the Al or Ti mask when electromigration is applied; furthermore, the glass is altered under the mask in such a way that subsequent ion exchanges are hinder (borosilicate glass) or prevented (soda-lime glass) in these regions [54]. This blocking effect was attributed to the appearance of a Na^+ depleted layer under the mask and a change of the glass structure therein. It was proved that dielectric masks do not cause such effects.

Silver reduction points out that the edge of Al mask acts as a cathode, which suggests that this boundary should be modelled as indicated in section 4.3. However, this does not explain the rest of the anomalies; in particular, the physical nature of the positive charge flowing from mask to glass is unclear. Briefly, although eq. (62) can be used to obtain approximate results, no satisfactory boundary conditions for metallic masks are still established.

5. Typical arrangements of waveguide fabrication

Common experimental arrangements of waveguide fabrication are analysed in this section. The validity of usual assumptions are checked by taking into account the above mentioned ideas.

5.1. *Multidimensional thermal ion exchange from a salt*

Let us consider a piece of glass whose side is masked with a dielectric substance. Mask openings can have arbitrary shapes in order to allow a selective ion exchange when the sample is immersed in a molten salt. The potential ϕ verifies

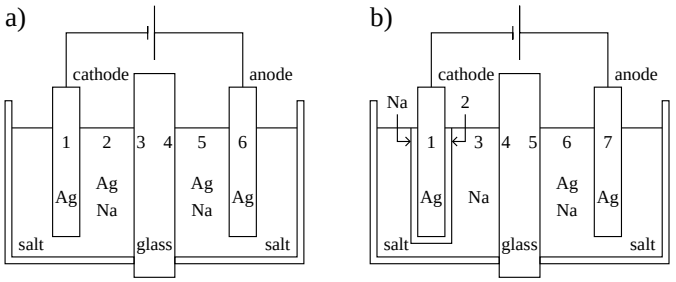

Fig. 1. Typical arrangement to perform electro-diffusion. a) silver and sodium cations at both sides. b) only sodium cations at the cathode side.

the boundary condition (65) at masked regions, whereas eq. (43) applies to the opened ones. Therefore the solution for ϕ is just the constant:

$$\phi(\vec{r},t) = \phi|_F \qquad \forall\, \vec{r},t \tag{66}$$

$\vec{r}$ being the position vector inside the glass piece and $\phi|_F$ is taken from eq. (43). This means —eq. (23)— that the total current is null regardless of the number of problem dimensions, as it is usually assumed. Thus, the ion diffusion is governed by the eq. (21) where the drift term disappears, resulting in a generalization of eq. (1) for a non-ideal cation behaviour.

In contrast, a total current surely exists when metallic masks are used; hence predictions, under the common assumption that total current is null, will be able to be improved when correct boundary conditions for metallic masks are established (see section 4.5), as it has already been suggested in [55].

5.2. *Field assisted ion exchange from salts: reduction and oxidation of silver*

Let us consider a typical arrangement to perform electro-diffusion such as that in figure 1a. It represents a glass sheet between two molten mixtures of salts. Each one of them has a different silver and sodium nitrate ratio. Moreover, there is a silver electrode inside each salt. In order to formalise the study, the different phases are numbered in a sequential way. Each side of the glass sheet has a different number because equilibrium is assumed everywhere except inside the glass. When a clockwise current is present in the circuit, silver atoms oxidate at phase 6 and pass into phase 5 whereas silver cations of phase 2 are reduced and aggregated to phase 1 as metallic silver. It is assumed, as in section 4.2, that there is enough silver in phase 2 to neglect sodium reduction. Therefore:

$$\begin{aligned} \mu_{\mathrm{Ag}^+1} &= \mu_{\mathrm{Ag}2} = \mu_{\mathrm{Ag}}|_3 \\ \mu_{\mathrm{Ag}^+6} &= \mu_{\mathrm{Ag}5} = \mu_{\mathrm{Ag}}|_4. \end{aligned} \tag{67}$$

By subtracting both equations, it is obtained:

$$V|_4 - V|_3 = V_6 - V_1 - \frac{k_{\mathrm{B}}T}{e}\ln\frac{a_{\mathrm{Ag}}|_4}{a_{\mathrm{Ag}}|_3} \tag{68}$$

and then, the difference between the values of ϕ at both surfaces is:

$$\phi|_4 - \phi|_3 = V_6 - V_1 + \frac{k_{\mathrm{B}}T}{e}\ln\frac{1+\left.\frac{D_{\mathrm{Na}}c_{\mathrm{Na}}}{D_{\mathrm{Ag}}c_{\mathrm{Ag}}}\right|_4}{1+\left.\frac{D_{\mathrm{Na}}c_{\mathrm{Na}}}{D_{\mathrm{Ag}}c_{\mathrm{Ag}}}\right|_3}. \tag{69}$$

It has been often assumed that the potential difference to calculate the current ($\phi|_4 - \phi|_3$) is the same as that applied ($V_6 - V_1$), but the last equation shows that this is exact only when both salts have the same composition (then $c_i|_3 = c_i|_4$). In general, the system acts as an electrochemical cell, for instance if both salts are short-circuited ($V_1 = V_6$) and $c_{\mathrm{Ag}}|_3 \neq c_{\mathrm{Ag}}|_4$, a current crosses the glass sheet. Inversely, when the external circuit is open there is no current ($J_0 = 0$), then $\phi|_3 = \phi|_4$ and a potential difference arises between both electrodes ($V_1 \neq V_6$) provided $c_i|_3 \neq c_i|_4$. Anyway, the correction is expected to be about tenths of volt, hence, it can be usually ignored.

5.3. *Field assisted ion exchange from salts: reduction and oxidation of different cation species*

When no silver cations are present at the left side salt, the equation (69) is not longer valid since sodium reduction occurs instead of silver reduction in the cathode. The new situation is showed in figure 1b, where a metallic sodium layer was considered on the cathode, which forces us to renumber the phases. A new equilibrium between silver cathode electrons and sodium layer electrons is assumed:

$$\mu_{e^-1} = \mu_{e^-2}, \tag{70}$$

where these electrochemical potentials are:

$$\begin{aligned} \mu_{e^-1} &= -W_{e^-}^{\mathrm{Ag}} - eV_1 \\ \mu_{e^-2} &= -W_{e^-}^{\mathrm{Na}} - eV_2, \end{aligned} \tag{71}$$

When electrochemical potentials of cations and electrons are added, a value independent of potentials results, that is:

$$\begin{aligned} \mu_{e^-1} + \mu_{\mathrm{Ag}^+1} &= -(W_{e^-}^{\mathrm{Ag}} + W_{\mathrm{Ag}^+}^{\mathrm{Ag}}) \\ \mu_{e^-2} + \mu_{\mathrm{Na}^+2} &= -(W_{e^-}^{\mathrm{Na}} + W_{\mathrm{Na}^+}^{\mathrm{Na}}). \end{aligned} \tag{72}$$

By subtracting both equations, taking into account the equilibrium between phases 2, 3 and 4:

$$\mu_{\mathrm{Na}^+2} = \mu_{\mathrm{Na}3} = \mu_{\mathrm{Na}}|_4 = \bar{\mu}_{\mathrm{Na}}^0 + eV|_4, \tag{73}$$

and finally using (29), it is obtained:

$$\begin{aligned} \phi|_5 - \phi|_4 = V_7 - V_1 &+ \frac{W_{e^-}^{\mathrm{Na}} + W_{\mathrm{Na}^+}^{\mathrm{Na}}}{e} - \frac{W_{e^-}^{\mathrm{Ag}} + W_{\mathrm{Ag}^+}^{\mathrm{Ag}}}{e} + \frac{\bar{\mu}_{\mathrm{Na}}^0 - \bar{\mu}_{\mathrm{Ag}}^0}{e} \\ &+ \frac{k_{\mathrm{B}}T}{e}\ln\left(\frac{D_{\mathrm{AgAg}}}{D_{\mathrm{NaNa}}} + \left.\frac{a_{\mathrm{Na}}}{a_{\mathrm{Ag}}}\right|_5\right). \end{aligned} \tag{74}$$

The two first fractions of right hand equation side amount to -4.3 V (table 1) and the last term takes usually small

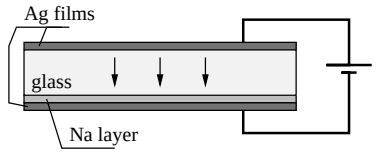

Fig. 2. Dry electro-diffusion arrangement

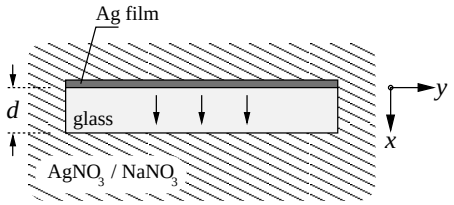

Fig. 3. Arrangement to make simultaneous ion exchange from a silver film and a mixture of molten salts

values. The third fraction probably is also negative, as it was already argued in section 4.3.2. Hence, when oxidation and reduction of different cation species occurs at each electrode, the electrochemical cell effect can achieve some Volts and therefore it should not be neglected any longer.

5.4. *Dry field-assisted diffusion*

Let us consider the system in the figure 2: a sheet of soda glass silvered on both sides. When a potential difference is applied between them, a film provides silver cations to the glass while sodium cations become metal under the opposite film. By assuming again an equilibrium between silver cathode electrons and sodium layer electrons —phases 1 and 2 in the eq. (70)—, and by using the eqs. (52) and (61), an equation identical to (74) is obtained. Thus, the same conclusions as in section 5.3 are drawn.

5.5. *Thermal silver diffusion from salt and film simultaneously*

Let us consider a sheet of homogeneous glass silvered on one side. Let us also consider this submerged in a molten mixture of silver and sodium nitrates (figure 3). The system can be assumed one-dimensional far from sheet edges. Thus, the boundary conditions for ϕ are given by the eqs. (52) at $x = 0$ and (43) at $x = d$, d being the sample thickness. Nevertheless, an extra relationship between V_s and V_f is needed, which is obtained from the equilibrium condition between silver cations from film and salt:

$$\mu_{\mathrm{Ag^+\,f}} = \mu_{\mathrm{Ag\,s}}. \tag{75}$$

Thus, it is obtained:

$$\phi|_{x=d} - \phi|_{x=0} = \frac{k_\mathrm{B}T}{e} \ln \frac{1 + \left.\frac{D_\mathrm{Na}c_\mathrm{Na}}{D_\mathrm{Ag}c_\mathrm{Ag}}\right|_{x=d}}{1 + \left.\frac{D_\mathrm{Na}c_\mathrm{Na}}{D_\mathrm{Ag}c_\mathrm{Ag}}\right|_{x=0}}. \tag{76}$$

Note the similarity with equation (69). Nevertheless, in this case, the variables evaluated at $x = 0$ change with time.

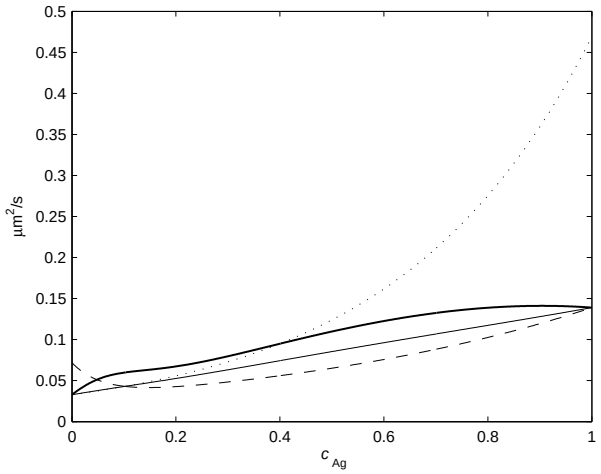

Fig. 4. D_Na (dashed), D_Ag (pointed), inter-diffusion coefficient (solid thick) and its mobility term (solid thin) at 360°C as reconstructed from [27].

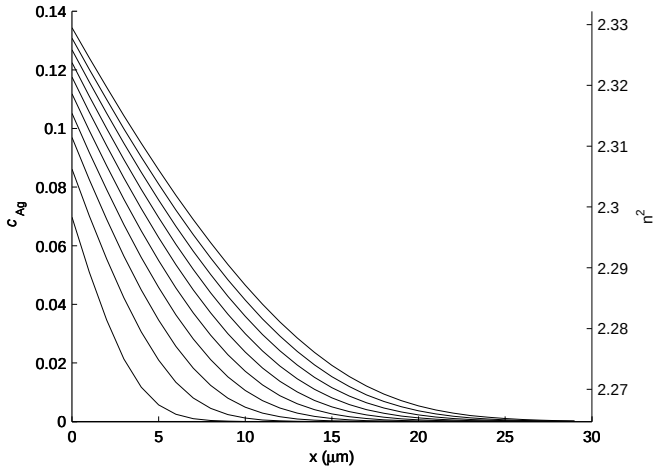

Fig. 5. Mole fraction profiles were calculated every 2 min under the silvered side of a glass sample when immersed in a molten mixture of silver and sodium nitrates. Right vertical axis shows the corresponding refractive index squared.

As it was said above, $\vec{J}_0$ only depends on time, since the problem is one-dimensional; thus, it is obtained by the integration of (23):

$$\frac{J_0}{C_0} = -\frac{\ln\left[1 + \frac{D_\mathrm{Na}c_\mathrm{Na}}{D_\mathrm{Ag}c_\mathrm{Ag}}\right]_{x=d} - \ln\left[1 + \frac{D_\mathrm{Na}c_\mathrm{Na}}{D_\mathrm{Ag}c_\mathrm{Ag}}\right]_{x=0}}{\int_0^d \frac{\mathrm{d}x}{D_A c_A + D_B c_B}} \tag{77}$$

where (76) was taken into account. The greater the difference of silver mole fractions on both sides of the sample, the larger the current. If mole fractions are equal on both sides ($c_\mathrm{Ag}|_{x=0} = c_\mathrm{Ag}|_{x=d}$), there is no current. For instance, if the glass sample is initially silver free ($c_\mathrm{Ag}|_{t=0} = 0 \;\forall\; x \in [0, d]$) and the molten salt does not contain silver (which implies that $c_\mathrm{Ag}|_{x=d} = 0 \;\forall\; t > 0$), then $J_0 = 0$ and $c_\mathrm{Ag} = 0 \;\forall\; x \in [0, d],\; t > 0$. This means, there is no silver crossing from film to glass.

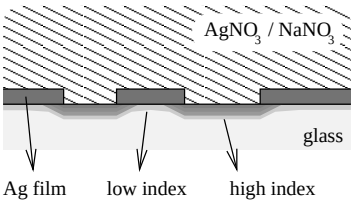

Fig. 6. Suggested method to fabricate optical integrated elements in a single step, by patterning a silver film.

To study a non-trivial and realistic case, the electro-diffusion problem was solved numerically by finite differences. The algorithm is similar to that used in [58]: linearly implicit Rosenbrock method, which is a generalisation for non-linear equations of the well-known Crank-Nicolson scheme. Nevertheless, this case is one-dimensional and it includes the current term unlike ref. [58]. The dependence of self-diffusion coefficients with mole fractions at 360°C for a sodium-containing boroaluminosilicate glass was extracted from [27] by fitting their experimental data from radioactive tracers to the functions:

$$\begin{aligned} D_{\mathrm{Ag}} &= D_0 \exp(\alpha_0 c_{\mathrm{Ag}}) \\ D_{\mathrm{Na}} &= D_1 \exp(\alpha_1 c_{\mathrm{Ag}}) + D_2 \exp(\alpha_2 c_{\mathrm{Na}}), \end{aligned} \tag{78}$$

which leads to $D_0 = 0.0328\ \mu\mathrm{m}^2/\mathrm{s}$, $D_1 = 0.0413\ \mu\mathrm{m}^2/\mathrm{s}$, $D_2 = 0.139\ \mu\mathrm{m}^2/\mathrm{s}$, $\alpha_0 = 2.66$, $\alpha_1 = -16.94$ and $\alpha_2 = -1.517$. These functions, the mobility term and the inter-diffusion coefficient are represented in figure 4. The latter was computed from D_{Ag} and D_{Na} under the assumption (28). Note the qualitative agreement with the experimental inter-diffusion coefficient of [27].

Let us consider a 0.17 mm thick glass sheet (like a microscope cover glass) with initial and boundary conditions for c_{Ag}:

$$\begin{aligned} &c_{\mathrm{Ag}}|_{t=0} = 0 \quad \forall\ x \in [0, d], \\ &c_{\mathrm{Ag}}|_{x=d} = 0.9\ \forall\ t > 0 \end{aligned} \tag{79}$$

and equation (47) at $x = 0$. Although this initial condition implies that the current diverges at $t = 0$, it is physically consistent since the amount of silver that enters into the glass during finite time is also finite. The profiles obtained under the film surface are represented for several diffusion times in figure 5. As silver mole fraction increases at $x = 0$, the current reduces strongly. For intermediate times, J_0 is small in comparison with the density currents of usual electro-diffusion experiments. This fact results in low profiles that evolve slowly. Both a thinner sample as a more pure silver nitrate salt could be used for increasing the current. The former reduces the sample resistance while the latter increases slightly the difference of values of ϕ on both sample sides. Finally, $c_{\mathrm{Ag}}|_{x=0}$ tends asymptotically to $c_{\mathrm{Ag}}|_{x=d}$ while J_0 tends to zero for very long diffusion times.

This result suggests the combination of silvered and open regions on the same side of the sample to fabricate integrated optical components such as lenses or channel waveguides in a single diffusion step (Figure 6). A low effective index profile will shape under the silvered region while the fundamental mode of the open region waveguide will have a high effective index. Thus, a refraction of guided light occurs at the transition, which can be used to fabricate integrated lenses or prisms. This method is attractive because it requires only one lithographic step and one diffusion step. Furthermore, we can use an experimental arrangement for thermal diffusion which is much simpler than the one necessary for field-assisted ion exchange. Of course, a two-dimensional study of both the index distribution of the transition and the optical propagation through this transition is needed, but this task is beyond the scope of this work.

6. Conclusions

The conventional equation of the mole fraction (c_A) is generalised for both non-ideal cation behaviour and self-diffusion coefficients that depend on c_A. The usual assumption of the Ohm's law leads to an inaccurate equation for the calculation of the electric potential (V). Instead, the Faraday equation must be imposed. Thus, the current density is obtained from the gradient of an effective electric potential ϕ. The difference between this potential and the true electric potential at a given point is a function of the mole fraction at that point. This function takes a simple form when each self-diffusion coefficient is assumed to be proportional to the respective activity coefficient, which is reasonable and includes the ideal case of constant self-diffusion coefficients as a particular case. Although the difference between V and ϕ only amounts some tenths of volt, their gradients differ notably where the gradient of c_A is large.

The glass boundary conditions with molten salts are obtained from standard electrolyte theory. The usual condition for c_A is recovered whereas a discontinuity in the electrical potential is obtained. This contact potential leads to a Dirichlet condition for ϕ that depends on the salt and glass mole fractions. The same theory is applied to obtain the boundary conditions with a metal film (usually silver) operating as a cation source. The usual mixed condition for c_A is generalised to a non-ideal behaviour. Again a contact potential arises between glass and film, but now $\phi|_{\mathrm{F}}$ can depend on the time and on the surface point through the c_A. That is, the film boundary conditions are coupled. When a metallic film acts as a cathode, a new metallic layer builds up under the film by reduction of cations from the glass. A contact potential also exists in this case. If two cation species are present at the glass surface, both the mole fraction of the layer and its contact potential with glass change with time.

As regards these results, some common configurations for field assisted ion exchange from salts were checked. It was shown that they behave as electrochemical cells. Therefore, the whole system, including anode and cathode, must be taken into account. If the specie that oxidises at the anode

is the same as that is reduced at the cathode, the difference of ϕ between both sample sides agrees with the applied voltage or the correction is proportional to $k_{\rm B}T/e$ and can be neglected compared with large applied voltages. Nevertheless, if these species are different, the correction can amount some Volts and should be retained.

Finally, it was predicted that the electrochemical cell effect can be used to diffuse cations from a silver film without need for an externally applied field. The resultant current for slab configuration is small after a short time. So the index profile is low, which results in propagation modes with low effective indexes. This suggests the combination of silvered and open regions to fabricate integrated optical components in a single diffusion step. The method seems attractive because it has only one lithographic step and one diffusion step; furthermore the experimental arrangement is as simple as that of a thermal diffusion.

7. Acknowledgements

The author thanks Dr. J. Liñares Beiras for valuable discussions and suggestions.

Appendix A. Flux density of cations

In order to justify the equation (11) and explain their physical meaning, first, a simplified version of Eiring's model of diffusion is assumed (see for example [59]). The derivation will be carried out for cations A; of course, an identical treatment can be made for cations B. Thus, it is assumed that most cations A and B are fixed in the glass network sites, whereas only a very small amount of them are moving from a site to another in an excited state. Hereafter, they will be called $\rm A^{\downarrow}$ and $\rm A^{\uparrow}$ to fixed and mobile cations A respectively. Therefore:

$$C_{A\downarrow} + C_{A\uparrow} = C_A \qquad C_{A\uparrow} \ll C_A \tag{A.1}$$

where $C_{A\downarrow}$ and $C_{A\uparrow}$ are the corresponding concentrations. Since the typical diffusion times are very large (minutes) compared with the life time of an excited state, it can be assumed that fixed and mobile cations are in equilibrium, which means that their electrochemical potentials ($\mu_{A\downarrow}$ and $\mu_{A\uparrow}$ respectively) are the same:

$$\mu_{A\downarrow} = \mu_{A\uparrow} \equiv \mu_A \tag{A.2}$$

Next, it is assumed that mobile cations do not interact with other mobile cations because of their low concentration; that is, they behave *ideally* in respect of other mobile cations:

$$\mu_{A\uparrow} = \bar{\mu}^0_{A\uparrow} + k_{\rm B}T \ln \frac{C_{A\uparrow}}{C_0} + eV, \tag{A.3}$$

although $\bar{\mu}^0_{A\uparrow}$ can depend on $C_{A\downarrow}$ and $C_{B\downarrow}$, and therefore it can be a function of the position and the time. As all cations, as a whole, could not behave ideally, we have:

$$\begin{aligned}\mu_A &= \bar{\mu}^0_A(C_A + C_B) + k_{\rm B}T \ln a_A(c_A) + eV \\ &\simeq \bar{\mu}^0_A(C_0) + k_{\rm B}T \ln a_A(c_A) + eV,\end{aligned} \tag{A.4}$$

where it was stressed that a_A is a function of the mole fraction whereas $\bar{\mu}^0_A$ depends on the absolute concentration because the ion exchange is performed one to one. Hereafter, such dependencies will be omitted. By using the last three equations, a relationship between $C_{A\uparrow}$ and a_A is obtained:

$$C_{A\uparrow} = a_A C_0 \exp \frac{\bar{\mu}^0_A - \bar{\mu}^0_{A\uparrow}}{k_{\rm B}T}. \tag{A.5}$$

On the other hand, the flux density of $\rm A^{\uparrow}$ cations (and therefore $\vec{J}_A$) must be proportional to the gradient of $\mu_{A\uparrow}$:

$$\begin{aligned}\vec{J}_A = \vec{J}_{A\uparrow} &= L_{A\uparrow} \vec{\nabla} \frac{\mu_{A\uparrow}}{k_{\rm B}T} \\ &= -D_{A\uparrow} \vec{\nabla} C_{A\uparrow} + \frac{e\vec{E} - \vec{\nabla}\bar{\mu}^0_{A\uparrow}}{k_{\rm B}T} D_{A\uparrow} C_{A\uparrow}\end{aligned} \tag{A.6}$$

where $L_{A\uparrow} = -D_{A\uparrow}C_{A\uparrow}$, being $D_{A\uparrow}$ the diffusion coefficient of mobile cations. Again, due to the low concentration of $\rm A^{\uparrow}$ cations, $D_{A\uparrow}$ is expected to depend only on the temperature. By defining the diffusion coefficient of the cations A as:

$$D_A \equiv D_{A\uparrow}\gamma_A \exp \frac{\bar{\mu}^0_A - \bar{\mu}^0_{A\uparrow}}{k_{\rm B}T} \tag{A.7}$$

it is obtained:

$$D_A C_A = D_{A\uparrow} C_{A\uparrow}, \tag{A.8}$$

being γ_A the thermodynamic activity coefficient ($a_A = \gamma_A c_A$), which leads to a flux equation that depends on C_A:

$$\vec{J}_A = -\vec{\nabla}\left(D_A C_A\right) + \frac{e\vec{E} - \vec{\nabla}\bar{\mu}^0_{A\uparrow}}{k_{\rm B}T} D_A C_A. \tag{A.9}$$

The usual expression for $\vec{J}_A$ is retrieved when the gradient term is expanded, which cancels the driving term proportional to $\vec{\nabla}\bar{\mu}^0_{A\uparrow}$:

$$\vec{J}_A = -D_A\left(1 + \frac{\partial \ln \gamma_A}{\partial \ln c_A}\right)\vec{\nabla} C_A + \frac{e\vec{E}}{k_{\rm B}T} D_A C_A \tag{A.10}$$

This expression could be obtained directly from (A.4), but the above procedure also provides the dependence of D_A (A.7). Experimental studies [26,27] showed that the term in parenthesis (the so called *thermodynamic term*) has a relevant contribution, which demonstrates a non-ideal behaviour of the cations as a whole. Such a dependence of γ_A explains, at least qualitatively, the behaviour of D_A as a function of c_A, indicating that $\bar{\mu}^0_{A\uparrow}$ has a weak dependence on mole fractions. Thus (28) approximates to (A.7), where:

$$D_A|_{c_A=1} \equiv D_{AA} \simeq D_{A\uparrow} \exp \frac{\bar{\mu}^0_A - \bar{\mu}^0_{A\uparrow}}{k_{\rm B}T}. \tag{A.11}$$

References

[1] R.V. Ramaswamy and R. Srivastava *J. Lightwave Technol.* 6 (1988) 984

[2] S.I. Najafi (ed) *Introduction to Glass Integrated Optics*, Artech House (Boston · London, 1992)

[3] F. Helferich and M.S. Plesset *The Journal of Chemical Physics* 28 (1958) 418

[4] M. Abou-el-Leil and A.R. Cooper *Journal of The American Ceramic Society* 62 (1979) 390

[5] H-J. Lilienhof, E. Voges, D. Ritter and B. Pantschew *IEEE J. Quantum Electron.* QE-18 (1982) 1877

[6] J. Albert and J.W.Y. Lit *Appl. Opt.* 29 (1990) 2798

[7] A. Tervonen *J. Appl. Phys.* 67 (1990) 2746

[8] A.J. Cantor, M. Abou el leil and R.H. Hobbs *Appl. Opt.* 30 (1991) 2704

[9] D. Cheng, J. Saarinen, H. Saarikoski and A. Tervonen *Opt. Commun.* 137 (1997) 233

[10] J. Hazart and V. Minier *IEEE J. Quantum Electron.* 37 (2001) 606

[11] B.R. West, P. Madasamy, N. Peyghambarian and S. Honkanen *J. Non-Cryst. Solids* 347 (2004) 18

[12] G. Eisenman *Biophysis. J.* 2 (1969) 259

[13] R.H. Doremus *Glass Science*, John Wiley & Sons Inc. (New York, 1994)

[14] E.A. Guggenheim *Thermodynamics*, Fifth Ed., Noth-Holland Publishing Company (Amsterdam, 1967)

[15] A. Quaranta, F. Gonella *J. Non-Cryst. Solids* 192&193 (1995) 334

[16] X. Prieto, R. Srivastava, J. Liñares, C. Montero *Opt. Mat.* 5 (1996) 145

[17] A. Lupascu, A. Kevorkian, T. Bondet, F. Saint-André, D. Persegol and M. Levy *Opt. Engineering* 35 (1996) 1603

[18] R. Teray and R. Hayami *J. Non-Cryst. Solids* 18 (1975) 217

[19] D.E. Day *J. Non-Cryst. Solids* 21 (1976) 343

[20] M.D. Ingram *Physics and Chemistry of Glasses* 28 (1987) 215

[21] H.M. Garfinkel *The Journal of Physical Chemistry* 72 (1968) 4175

[22] P. Chludzinski, R.V. Ramaswamy, and T.J. Anderson *Physics and Chemistry of Glasses* 28 (1987) 169

[23] R. Araujo *J. Non-Cryst. Solids* 152 (1993) 70

[24] J.M. Inman, J.L. Bentley, and S.N. Houde-Walter *J. Non-Cryst. Solids* 191 (1995) 209

[25] J. Liñares, K. Siva Rama Krishna and M.C. Nistal, *Appl. Opt.* 36 (1997) 6838

[26] H. Wakabayashi *J. Non-Cryst. Solids* 203 (1996) 274

[27] B. Messerschmidt, C.H. Hsieh, B.L. McIntyre and S.N. Houde-Walter *J. Non-Cryst. Solids* 217 (1997) 264

[28] T. Izawa and H. Nakagome *Appl. Phys. Lett.* 21 (1972) 584

[29] V. Newman, O. Parriaux and L.M. Walpita *Electron. Lett.* 15 (1979) 704

[30] J.L. Jackel *Appl. Opt.* 27 (1988) 472

[31] J.E. Samuels and D.T. Moore *Appl. Opt.* 29 (1990) 4042

[32] N. Haun, D.S. Kindred, and D.T. Moore *Appl. Opt.* 29 (1990) 4056

[33] P.G. Noutsios and G.L. Yip *Appl. Opt.* 31 (1992) 5283

[34] T. Fϕrland *Fused Salts*, McGraw-Hill Book Co. (New York, 1964)

[35] V. Rothmund and G. Kornfeld *Z. Anorg. Allg. Chem.* 103 (1918) 129

[36] G.H. Chartier, P. Jaussaud, A.D. de Oliveira and O. Parriaux *Electron. Lett.* 14 (1978) 132

[37] C.W. Pitt, A.A. Stride and R.I. Trigle *Electron. Lett.* 16 (1980) 701

[38] K. Forrest, S.J. Pagano and W. Viehmann *J. Lightwave Technol.* LT-4 (1986) 140

[39] Bl. Pantchev *Opt. Comm.* 60 (1986) 373

[40] B. G. Pantchev *Electron. Lett.* 23 (1987) 1188

[41] S. Honkanen, A. Tervonen, H. von Bagh, A. Salin and M. Leppihalme *Appl. Phys. Lett.* 51 (1987) 296

[42] S. Honkanen and A. Tervonen *J. Appl. Phys.* 63 (1988) 634

[43] P. Pöyhönen, S. Honkanen, A. Tervonen, M. Tahkokorpi, J. Albert *Electron. Lett.* 27 (1991) 1319

[44] S.S. Gevorgyan *Electron. Lett.* 26 (1990) 38

[45] H. Márquez, D. Salazar, A. Villalobos, G. Paez, and J. Ma. Rincón *Appl. Opt.* 34 (1995) 5817

[46] F. Gonella, P. Canton, E. Cattaruzza, A. Quaranta, C. Sada, A. Vomiero *Mater. Sci. Eng. C* 29 (2006) 1087

[47] C. Kittel *Introduction to Solid state Physics*, Sixth Edition, John Wiley & Sons Inc. (New York, 1986)

[48] N.W. Ashcroft and N.D. Mermin *Solid State Physics*, Saunders College Publishers (Fort Worth, 1976)

[49] W.G. Moffatt *The Handbook of Binary Phase Diagrams* Genium Publishing Corporation (Schenectady, New York 1990)

[50] P. Villars (ed.-in-chief), H. Okamoto and K. Cenzual (section ed.) *http://www.asminternational.org/AsmEnterprise/APD*, ASM International, Materials Park, OH, 2006.

[51] B. Pantchev and P. Danesh *Jpn. J. Appl. Phys.* 36 (1997) 4320

[52] R. Walker, C.D.W. Wilkinson and J.A.H. Wilkinson *Appl. Opt.* 22 (1983) 1923

[53] M.N. Weiss and R. Srivastava *Appl. Opt.* 34 (1995) 455

[54] B. Pantchev, P. Danesh, and Z. Nikolov *Appl. Phys. Lett.* 62 (1993) 1212

[55] R-P. Salmio, J. Saarinen, J. Turunen, A. Tervonen *Appl. Opt.* 36 (1997) 2048

[56] R-P. Salmio, H. Saarikoski, J. Saarinen, J. Westerholm, and J. Turunen *Opt. Lett.* 22 (1997) 591

[57] A. Tervonen and S. Honkanen *Appl. Opt.* 35 (1996) 6435

[58] H. Saarikoski, R-P. Salmio, J. Saarinen, T. Eirola and A. Tervonen *Optics Communications* 134 (1997) 362

[59] T. L. Hill *An introduction to statistical thermodynamics*, Addison-Wesley (Massachussetts, 1962)